Article

Unraveling the Mechanisms Involved in the Beneficial Effects of Magnesium Treatment on Skin Wound Healing

Yuta Yoshino, Tatsuki Teruya, Chika Miyamoto, Mai Hirose, Satoshi Endo [ID] and Akira Ikari *[ID]

Laboratory of Biochemistry, Department of Biopharmaceutical Sciences, Gifu Pharmaceutical University, Gifu 501-1196, Japan; yoshino-yu@gifu-pu.ac.jp (Y.Y.); 175076@gifu-pu.ac.jp (T.T.); 195119@gifu-pu.ac.jp (C.M.); 195105@gifu-pu.ac.jp (M.H.); sendo@gifu-pu.ac.jp (S.E.)
* Correspondence: ikari@gifu-pu.ac.jp; Tel.: +81-58-230-8124

Abstract: The skin wound healing process consists of hemostatic, inflammatory, proliferative, and maturation phases, with a complex cellular response by multiple cell types in the epidermis, dermis, and immune system. Magnesium is a mineral essential for life, and although magnesium treatment promotes cutaneous wound healing, the molecular mechanism and timing of action of the healing process are unknown. This study, using human epidermal-derived HaCaT cells and human normal epidermal keratinocyte cells, was performed to investigate the mechanism involved in the effect of magnesium on wound healing. The expression levels of epidermal differentiation-promoting factors were reduced by $MgCl_2$, suggesting an inhibitory effect on epidermal differentiation in the remodeling stage of the late wound healing process. On the other hand, $MgCl_2$ treatment increased the expression of matrix metalloproteinase-7 (MMP7), a cell migration-promoting factor, and enhanced cell migration via the MEK/ERK pathway activation. The enhancement of cell migration by $MgCl_2$ was inhibited by MMP7 knockdown, suggesting that $MgCl_2$ enhances cell migration which is mediated by increased MMP7 expression. Our results revealed that $MgCl_2$ inhibits epidermal differentiation but promotes cell migration, suggesting that applying magnesium to the early wound healing process could be beneficial.

Keywords: keratinocyte; magnesium; matrix metalloproteinase; migration; wound healing

1. Introduction

The skin is the largest organ in the human body, which not only feels warmth and stimuli but also functions as a physical barrier between the internal and external sides of the organism, protecting against water loss from the body and the invasion of pathogens from the outside [1]. The skin has a three-layer structure consisting of the epidermis, dermis, and subcutaneous adipose tissue. The epidermis is the thickest layer containing keratinocytes and melanocytes, and it comprises four layers including the basal layer, spinous layer, granular layer, and stratum corneum [2]. Keratinocytes, which divide in the basal layer, lose their mitotic potential and differentiate as they move to the upper epidermal layers. After reaching the stratum corneum, the cells that have completed their final differentiation serve as a coating and protection for the body surface and eventually detach from the body surface [3].

When the skin is damaged physically, a complex cellular response called "wound healing" is initiated to maintain homeostasis by restoring the injured area to its pre-injury state. The process of skin wound healing is divided into in four stages as follows: the hemostatic, inflammatory, proliferative, and remodeling stages [4]. In the hemostatic stage, platelets assemble the surrounding blood cells to form a fibrin clot, covering the wounded region. Platelets then release growth factors and cytokines such as platelet-derived growth factors, leading to migration of the immune system cells and fibroblasts [4]. Subsequently, within hours of formation of the covered wound, the inflammatory phase

involves exudate and infiltration by the immune system cells [5]. The immune system cells produce proteases and reactive oxygen species to defend the wound area against external contaminants including bacteria [6]. In addition, growth factors and cytokines over-produced by immune system cells enhance cell migration and the proliferation of keratinocytes and fibroblasts at the wound edge [7]. Epidermal keratinocytes migrate according to the wound edge by degrading the extracellular matrix through the effect of plasminogen [8] and matrix metalloproteinases (MMPs) [9]. Fibroblasts proliferate in the wound area, leading to the production of extracellular matrix components, such as collagen, fibronectin, elastin, and hyaluronan and the formation of granulation tissue containing nerve fibers and capillaries. In the remodeling phase, epidermal keratinocytes differentiate to form the stratum corneum [10]. Repeated synthesis and catabolism of collagen in the granulation tissue result in a maturing scar and spontaneous regression of the granulation tissue back to its pre-injured state [7].

Delayed inflammatory and proliferative phases increase the risk of developing bacterial skin infections, and delayed epidermal differentiation during the remodeling stage also reduces patient quality of life by causing pain and wound appearance problems such as keloids and hypertrophic scars [11,12]. Thus, each stage in the wound healing process is regulated strictly. Factors that delay wound healing include diabetes, nutritional deficiencies, immunodeficiency, aging, and bacterial infection in the wound area.

The magnesium ion (Mg^{2+}) is an essential metal ion in the human body, and Mg^{2+} homeostasis is vital to maintaining the human health [13]. Mg^{2+} concentrations in vivo are regulated within a narrow range of 0.7–1.0 mM in healthy individuals. These concentrations are maintained by uptake from the gastrointestinal tract and excretion from the kidneys [13,14]. Mg^{2+} has a diverse range of physiological activities, alone or in concert with biomolecules. For example, Mg^{2+} is a cofactor for approximately 600 enzymes and an activator for more than 200 enzymes [13]. The hydrolysis of ATP by ATPases requires the complex formation of Mg^{2+} and ATP [15]. Therefore, Mg^{2+} is essential for various cellular responses including cell proliferation, cell cycle, and protein synthesis by both direct and indirect functions [16–18].

We reported that Mg^{2+} treatment of epidermal keratinocytes increases the expression of hyaluronic acid synthase via glycogen synthase kinase 3 and the cyclic AMP response element binding protein, resulting in increased hyaluronic acid production, which promotes wound healing [19]. We also demonstrated that Mg^{2+} treatment increases polyamine synthesis and reduces ultraviolet (UVB)-induced cell death in keratinocytes [20]. The above reports suggest that Mg^{2+} treatment may have several beneficial effects on epidermal keratinocytes. In addition, other researchers have reported that Mg^{2+} treatment promotes skin wound healing [21,22]. For example, treatment of hairless mouse skin wound sites with magnesium chloride ($MgCl_2$) promotes skin barrier function repair [21]. Applying a hydrogel releasing Mg^{2+} and Zn^{2+} into the back skin of mice promotes wound healing by promoting extracellular matrix reorganization via a fibroblast epithelial–mesenchymal transition [22]. From the above studies, it can be seen that Mg^{2+} promotes cutaneous wound healing and thus has valuable applications in wound care technology. However, it needs to be fully understood which wound healing processes require Mg^{2+}.

In this study, we investigated the effects of $MgCl_2$ treatment on cell migration and epidermal differentiation using the human epidermal keratinocyte cell line HaCaT cells and primary cultured normal human epidermal keratinocyte (NHEK) cells.

2. Results

2.1. Effect of Mg^{2+} on the Expression Levels of Epidermal Differentiation-Promoting Factors

To clarify the effects of $MgCl_2$ treatment on epidermal differentiation, differentiation-promoting factors, Tumor protein p63 (TP63), Desmoglein 3 (DSG3), Late Cornified Envelope 1E (LCE1E), FOS Like 2 (FOSL2), Wnt Family Member 5A (WNT5A), Semaphorin (SEMA) 3C, and SEMA5A mRNA expression levels were analyzed using real-time polymerase chain reaction (PCR). The results show that $MgCl_2$ treatment for 8 h significantly

reduces all epidermal differentiation mRNA expression levels (Figure 1A). Filaggrin, keratin 1, loricrin, and involucrin, used as epidermal differentiation markers, were also examined and all markers show suppression of expression (Figure 1B). In addition, significant suppression of keratin 1 and loricrin expressions by the $MgCl_2$ treatment was also observed in normal human epidermal keratinocytes (NHEK). Filaggrin and involucrin showed a similar trend toward expression suppression, although the effects were not statistically significant. These results indicated that Mg^{2+} may inhibit epidermal differentiation.
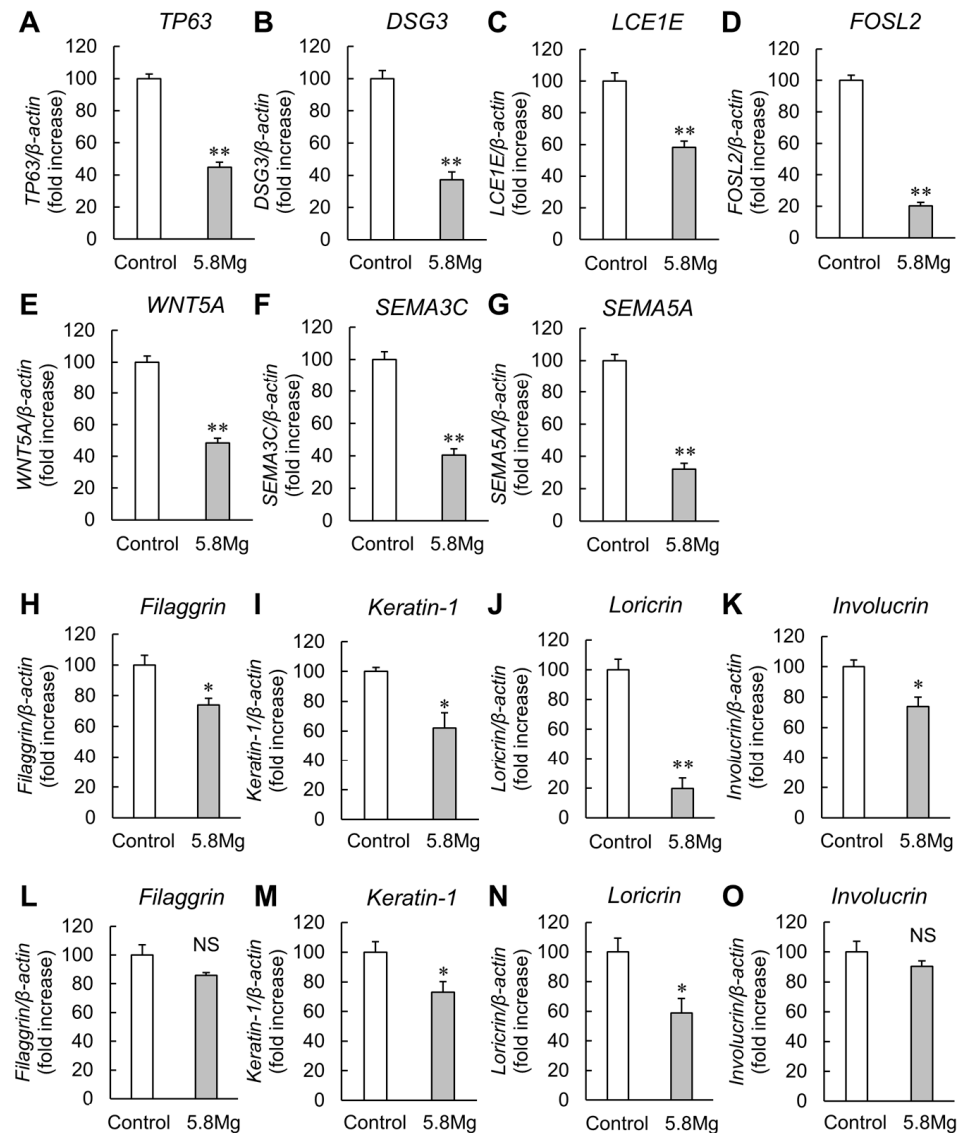

Figure 1. Effect of Mg^{2+} on the expression levels of keratinocyte differentiation-related genes. (**A–K**) HaCaT cells were cultured with DMEM containing 0.8 mM $MgCl_2$ (Control) and 5.8 mM $MgCl_2$ (5.8Mg) for 8 h. RT-PCR analysis showed the mRNA levels of (**A**) *TP63*, (**B**) *DSG3*, (**C**) *LCE1E*, (**D**) *FOSL2*, (**E**) *WNT5A*, (**F**) *SEMA3C*, (**G**) *SEMA5A*, (**H**) *filaggrin*, (**I**) *keratin-1*, (**J**) *loricrin*, (**K**) *involucrin*, and *β-actin*. $n = 4$. ** $p < 0.01$, vs. Control. (**L–O**) NHEK cells were cultured with Control and 5.8 $MgCl_2$ for 8 h. RT-PCR analysis showed the mRNA levels of (**L**) *filaggrin*, (**M**) *keratin-1*, (**N**) *loricrin*, (**O**) *involucrin*, and *β-actin*. $n = 4$. ** $p < 0.01$, * $p < 0.05$, NS $p > 0.05$, vs. Control.

2.2. Effects of Mg^{2+} on Cell Migration

A scratch assay was used to analyze the effect of both $MgCl_2$ and $MgSO_4$ on cell migration. The initial wound area was comparable, whereas the wound healing area increased in an $MgCl_2$ concentration-dependent manner after 12 h (Figure 2A,B). In addition, to

determine whether the migration-promoting ability was due to Mg^{2+}, cell migration ability after $MgSO_4$ treatment was also examined similarly. Treatment with $MgSO_4$ significantly enhances cell migration, like $MgCl_2$ (Figure 2C,D). The results indicate that Mg^{2+} enhances cell migration capacity.
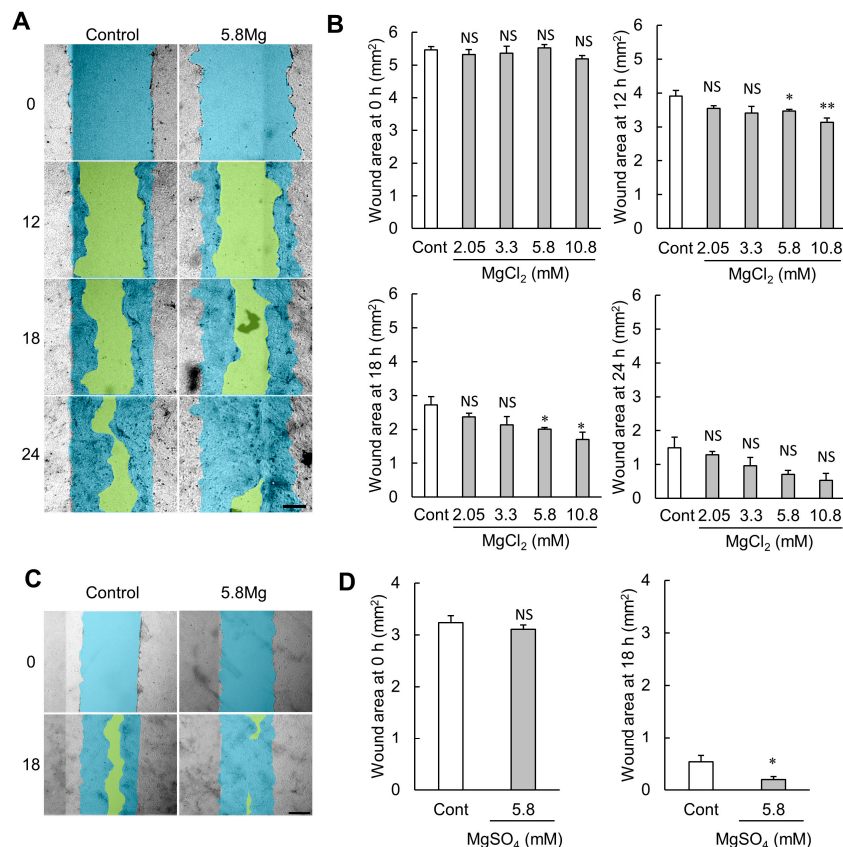

Figure 2. Effect of Mg^{2+} on cell migration. (**A–D**) HaCaT cells were cultured in 24 well plates until confluent and scratched with a pipette tip. Then, the cells were cultured in 0.5% FBS medium supplemented with 0.8–10.8 mM $MgCl_2$ (**A,B**) or 5.8 mM $MgSO_4$ (**C,D**). (**A**) The typical images of the cells with DMEM containing 0.8 mM $MgCl_2$ and 5.8 mM $MgCl_2$ are presented. (**B**) The scratched area was examined as a wound healing area (mm^2) in each time point. $n = 4$. (**C**) Typical images of the cells with 5.8 mM $MgSO_4$ are presented. (**D**) The scratched area was examined as a wound healing area (mm^2) in 18 h. $n = 4$. ** $p < 0.01$, * $p < 0.05$, NS $p > 0.05$ vs. Control. Yellow shows the wounded area. Blue shows the initial wounded area.

2.3. Effect of Mg^{2+} on Cytoskeletal Rearrangement

As $MgCl_2$ treatment enhanced the migratory capacity of HaCaT cells, the mechanism of this enhancement was investigated. Then, the effect of $MgCl_2$ treatment on extracellular signal-regulated kinase (ERK) 1/2 phosphorylation was investigated using Western blotting. The results show that treatment with 5.8 mM $MgCl_2$ markedly increases the phosphorylation levels of ERK1/2 (Figure 3A). Then, we analyzed $MgCl_2$ treatment on cytoskeletal changes that occur in the early stages of migration by F-actin staining using phalloidin. This probe stains only polymerized actin (Figure 3B). The results show that $MgCl_2$ treatment does not significantly change the intensity or morphology of the F-actin signal. Then, we performed a Western blotting analysis using an intracellular Ca^{2+} chelator to examine whether $MgCl_2$ promotes the phosphorylation of ERK1/2 by altering intracellular Ca^{2+} influx. Under treatment with BAPTA-AM, $MgCl_2$ significantly increased the phosphorylation of ERK (Figure 3C), suggesting that changes in Ca^{2+} influx may not exert $MgCl_2$-induced activation of ERK. On the other hand, the downstream factor of MEK/ERK-induced cell proliferation *cyclin D1 (CCND1)* mRNA did not change by treat-

ment with MgCl$_2$ (Figure 3D), suggesting that MgCl$_2$ may not promote cell proliferation. The above results indicate that MgCl$_2$ treatment enhances ERK1/2 phosphorylation, an intracellular signaling factor required for cell migration, but may promote cell migration by a mechanism other than cytoskeletal reorganization by polymerized actin.
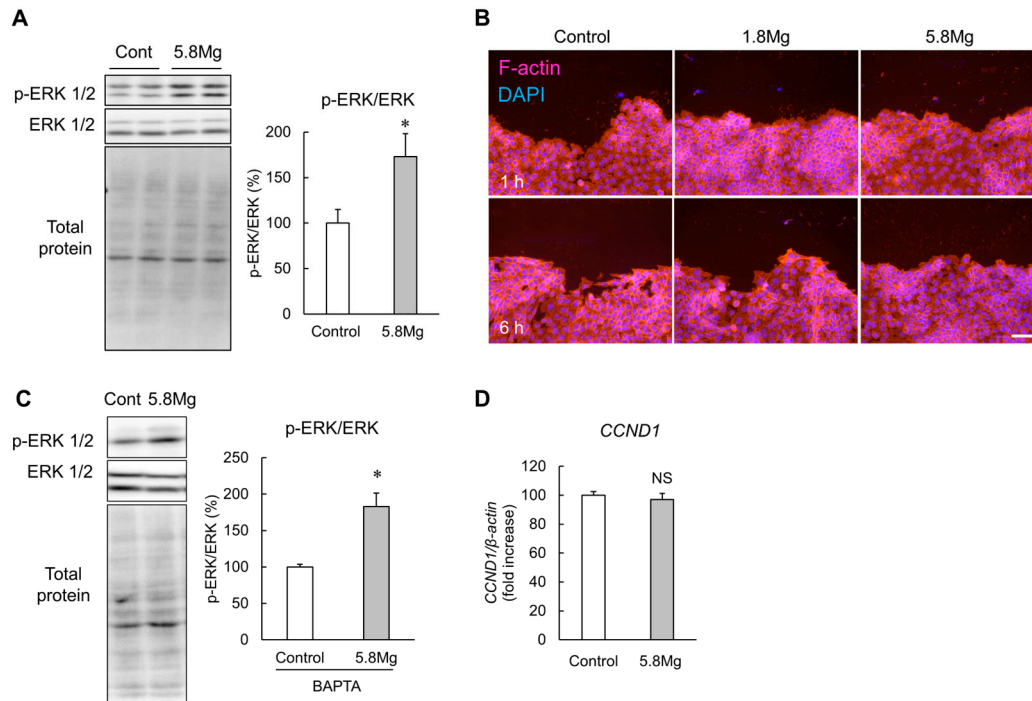

Figure 3. Effect of Mg^{2+} on cytoskeletal rearrangement. (**A**) HaCaT cells were cultured with DMEM containing 0.8 mM MgCl$_2$ (Control) and 5.8 mM MgCl$_2$ (5.8 Mg) for 1.5 h. Phosphorylated-ERK1/2 and total ERK1/2 protein levels were analyzed using Western blotting. n = 4–6. * p < 0.05 vs. Control. (**B**) HaCaT cells were cultured with Control and 5.8Mg for 0, 1, and 6 h after scratching with a pipette tip. The cells were observed using a fluorescence microscope after staining with Rhodamine Phalloidin (F-actin, red) and DAPI (nuclear, blue). Scale bar = 100 μm. (**C**) HaCaT cells were cultured with Control and 5.8Mg with 50 μM BAPTA-AM for 1.5 h. Phosphorylated-ERK1/2 and total ERK1/2 protein levels were analyzed using Western blotting. n = 4. * p < 0.05 vs. Control. (**D**) HaCaT cells were cultured with DMEM containing and 5.8 mM for 8 h. RT-PCR analysis showed the mRNA levels of *cyclin D1 (CCND1)* and *β-actin*. n = 4. NS p > 0.05 vs. Control.

2.4. Effect of Mg^{2+} on MMPs Expression

Next, a real-time PCR analysis was performed to investigate the effect of MgCl$_2$ treatment on the expression levels of MMP mRNA, and downstream factors of the ERK1/2 pathway. The results showed that MgCl$_2$ treatment increased *MMP1* and *MMP7* mRNA expression levels (Figure 4A); the increase in *MMP7* mRNA expression levels by MgCl$_2$ treatment was also observed in NHEK cells (Figure 4B). In contrast, *MMP1* mRNA expression levels were unchanged in NHEK cells; Western blotting analysis showed that MMP7 protein levels were increased by MgCl$_2$ treatment (Figure 4C). Analysis of MMP7 protein localization by fluorescence immunostaining showed a stronger MMP7 protein signal with MgCl$_2$ treatment (Figure 4D). Next, the MEK inhibitor was used to clarify the possibility of the MEK/ERK signal, a key pathway in cell signaling, regulating the MMP7 expression. Pretreatment with U0126, an MEK inhibitor, repressed the Mg^{2+}-induced upregulation of MMP7 (Figure 4E). This suggests that the MEK/ERK signaling pathway is involved in the up regulation of MMP7, and its inhibition can prevent this process.
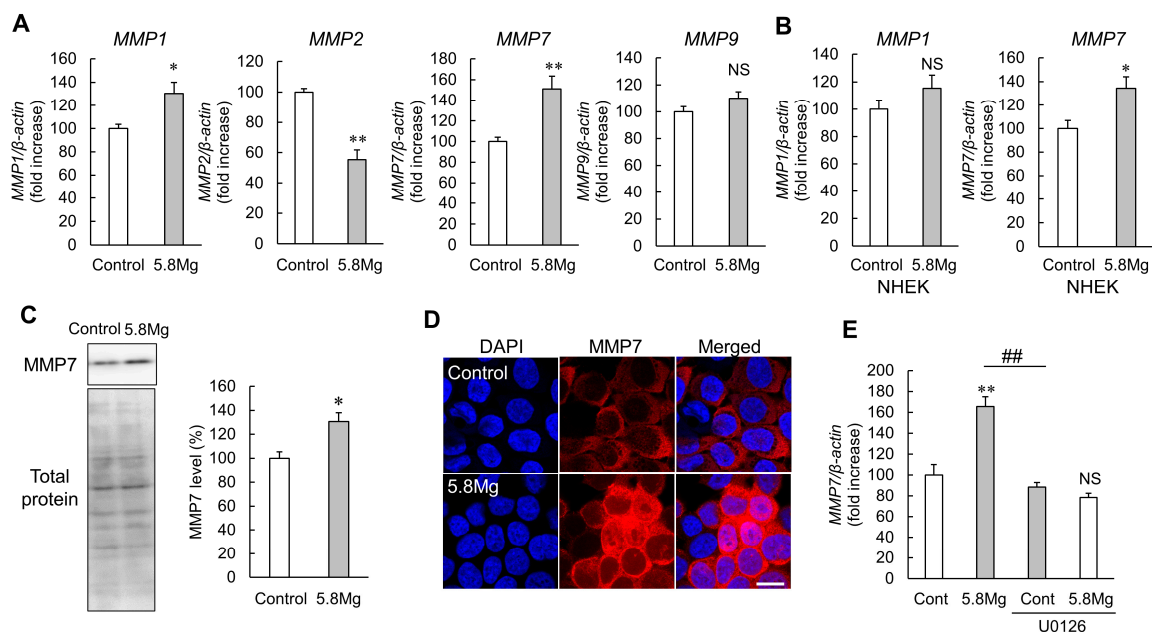
Figure 4. Effect of Mg^{2+} on MMPs expression. (**A**) HaCaT cells were cultured with DMEM containing 0.8 mM MgCl$_2$ (Control) and 5.8 mM MgCl$_2$ (5.8Mg) for 8 h. RT-PCR analysis showed the mRNA levels of *MMP1*, *MMP2*, *MMP7*, *MMP9*, and *β-actin*. (**B**) NHEK cells were cultured with Control and 5.8 Mg for 6 h. RT-PCR analysis showed the mRNA levels of *MMP1*, *MMP7*, and *β-actin*. (**C**) HaCaT cells were cultured in serum-free medium supplemented with Control and 5.8 Mg for 24 h. Western blotting analysis showed the protein level of MMP7. *n* = 4. ** *p* < 0.01, * *p* < 0.05, NS *p* > 0.05 vs. Control. (**D**) HaCaT cells were cultured on a cover glass with Control and 5.8Mg for 24 h. The cells were observed using confocal laser microscopy after staining with anti-MMP7 antibody (MMP7, red) and DAPI (nuclear, blue). Scale bar = 10 μm. (**E**) HaCaT cells were cultured with Control and 5.8 Mg with/or without 20 μM U0126 for 8 h. RT-PCR analysis showed the mRNA levels of *MMP7* and *β-actin*. *n* = 3–4. ** *p* < 0.01, NS *p* > 0.05 vs. Control. ## *p* < 0.01 vs. 5.8 Mg.

2.5. Effect of MMP7 Knockdown on Mg^{2+}-Induced Cell Migration Promotion

To clarify whether MMP7 expression contributes to MgCl$_2$-induced cell migration, MMP7 knockdown analysis was performed. In Western blotting analysis, MMP7 knockdown markedly reduced MMP7 protein expression (Figure 5A). Next, scratch assays in MMP7 knockdown cells were performed to investigate the effect of MgCl$_2$ treatment on cell migration capacity. As a result, the cell migration-promoting effect of MgCl$_2$ treatment seen in Figure 2 is not observed in MMP7 knockdown cells (Figure 5B). These results indicate that an increase in MMP7 protein expression mediates the cell migration-promoting effect of Mg^{2+}.
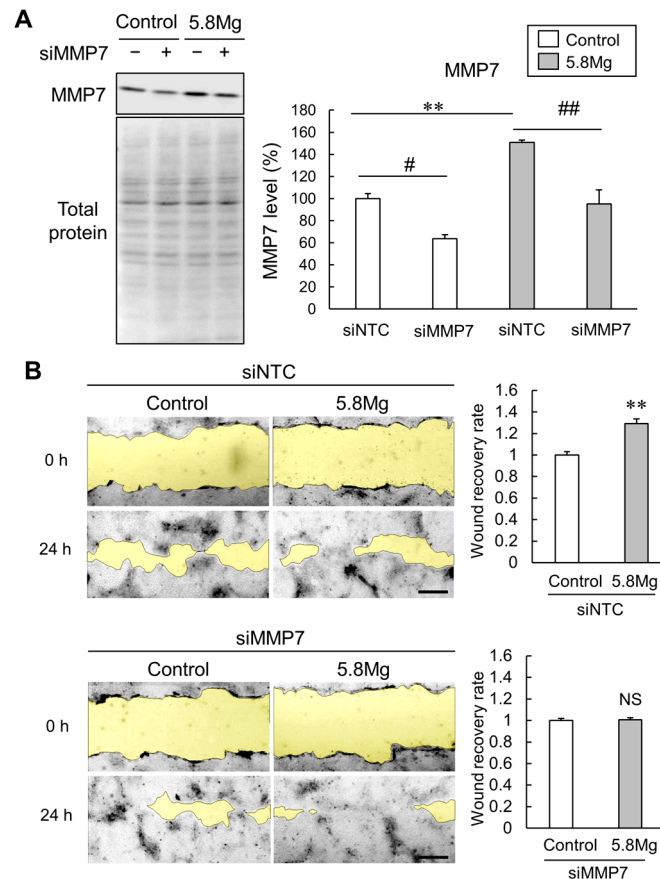
Figure 5. Effect of MMP7 knockdown on Mg^{2+}-induced cell migration promotion. (**A,B**) HaCaT cells transfected with 50 nM siRNA for a negative control (siNTC) and with MMP7 (siMMP7) were cultured for 48 h to knockdown the expression of MMP7. (**A**) HaCaT cells were cultured with DMEM containing 0.8 mM MgCl$_2$ (Control) and 5.8 mM MgCl$_2$ (5.8 Mg) for 24 h after MMP7 knockdown. After collecting the cells, MMP7 protein levels were analyzed using Western blotting. $n = 4$. ** $p < 0.01$, vs. siNTC control. ## $p < 0.01$, # $p < 0.05$ vs. siNTC. (**B**) The cells were cultured in 0.5% FBS medium supplemented with Control and 5.8 Mg conditions and scratched with a pipette tip after MMP7 knockdown. The typical images of the cells are presented. Yellow shows the wounded area. The scratched area is examined for the wound recovery rate (ratio to control) at 24 h. $n = 4$. NS $p > 0.05$ vs. Control.

3. Discussion

During the reconstructive phase of skin wound healing, epidermal keratinocytes are restored in functionally normal skin by appropriate differentiation [4,7,10]. Epidermal differentiation is regulated by various differentiation-related factors, including epidermal differentiation-promoting factors such as TP63, promoting epidermal stratification and cell adhesion [23,24]; DSG3, involved in growth inhibition and intercellular adhesion [25]; LCE1E [26] and FOSL2 [27], regulators of final epidermal differentiation and functioning in activating protein-1; and WNT5A, involved in inhibiting the WNT pathway, which is required for follicle formation and promotion of epidermal growth and differentiation. WNT5A, SEMA3C, and 5A are involved in nerve axon guidance and angiogenesis [28,29]. Filaggrin is a moisturizing factor of cornified envelopes [30]. Expression of the epidermal marker Keratin-1 is restricted to an intermediate stage of terminal differentiation [31]. Loricrin and involucrin are epidermal terminal differentiation factors [32,33]. The expression levels of all keratinocyte differentiation-related factors examined in the current study are decreased by MgCl$_2$ treatment, suggesting that Mg^{2+} has an inhibitory contribution to epidermal re-differentiation in the late stages of skin wound healing.

During the proliferative phase of wound healing, epidermal keratinocyte migration, which occludes the wound edge, is an essential phenomenon [10]. In the present study, $MgCl_2$ treatment enhances cell migration capacity in the scratch assay (Figure 2), suggesting that Mg^{2+} promotes wound healing during the early stages of healing when cell migration is required to seal the wound. Activation of ERK is essential for the migratory abilities of epidermal cells [34]. In the present study, phosphorylation of ERK is increased by $MgCl_2$ treatment (Figure 3A). During cell migration, cytoskeletal reorganization occurs, forming leaf-like pseudopodia, filamentous pseudopodia, and stress fibers composed mainly of actin filaments [35]. ERK1/2 phosphorylation is known to be involved in this cytoskeletal reorganization [36]. However, F-actin is not changed by $MgCl_2$ treatment (Figure 3B). The above results indicate that $MgCl_2$ treatment enhances ERK1/2 phosphorylation, an intracellular signaling factor required for cell migration, but may promote cell migration by a mechanism other than cytoskeletal reorganization by polymerized actin. MMPs, proteases which are involved in extracellular matrix degradation, are known to play an important role in epidermal keratinocyte migration [9]. Multiple MMP subfamilies have also been reported to be downstream factors of the ERK1/2 pathway [37–39]. In the present study, $MgCl_2$ treatment increases both protein and mRNA levels of MMP7 by activating the MEK/ERK pathway (Figure 4). Moreover, silencing MMP7 expression suppresses $MgCl_2$ treatment-induced cell migration (Figure 5). These findings suggest that Mg^{2+} may promote keratinocyte migration by activating the MEK/ERK/MMP7 axis to promote wound healing. However, considering the effects of Mg^{2+} on differentiation, applying $MgCl_2$ treatment to promote wound healing should not be limited to the entire wound healing process but only to the inflammatory phase when the inflammatory response is active and the proliferative phase when epidermal keratinocytes occlude the wound.

The physiological function of Mg^{2+} in cell differentiation differs between cell types. For example, Mg^{2+} promotes differentiation in osteoclasts and, conversely, inhibits differentiation in osteoblasts and skeletal muscle cells [40,41]. On the other hand, calcium ions (Ca^{2+}) are differentiation-promoting factors in various tissues, including the epidermis [42]. In the epidermis, Mg^{2+} inhibits Ca^{2+} influx, so intracellular Ca^{2+} levels decrease with the increasing intracellular Mg^{2+} levels [43]. This report suggests that Mg^{2+} inhibits differentiation. It has also been reported that increased ERK1/2 phosphorylation in the epidermis suppresses epidermal differentiation [44], which is consistent with the suppressive effect of $MgCl_2$ on the expression of epidermal differentiation-promoting factors observed in this study (Figure 1). The detailed mechanisms of ERK1/2 activation and epidermal differentiation suppression by Mg^{2+} are unknown and therefore require further analysis. In addition, as chronic enhancement of MMP expression has been reported to inhibit normal epidermal reconstitution and delay wound healing [45], the MMP7-enhancing effect of $MgCl_2$ treatment may have an inhibitory effect on epidermal reconstruction.

MMP7 is a low-molecular-weight enzyme found in the uterus [46], and its physiological function in normal skin has not been previously reported. As $MgCl_2$ promotes cell migration via increasing MMP7 expression (Figures 2 and 5), MMP7 in the epidermis may be a dominant factor for physiologic keratinocyte migration. However, the mechanism of the detailed cell migration-promoting effect of MMP7 is still unclear. In a previous report using lung cells, MMP7 degraded a type of extracellular matrix syndecan-1, which is a substrate for MMP7, and reduced integrin affinity, thereby promoting cell migration [47]. MMP7 in the skin may also promote cell migration by a similar mechanism, and integrin expression and activity should also be investigated in the future. It has also been reported that Mg^{2+} enhances ERK1/2 phosphorylation [48]. We demonstrated that ERK1/2 phosphorylation enhances MMP7 expression (Figure 4E). However, it remains unknown how Mg^{2+} activates the MEK/ERK pathway and as such, further studies are needed.

Current treatments for skin wounds include debridement, electrical stimulation, and hyperbaric oxygen therapy, but there are issues such as invasiveness and the risk of oxygen intoxication [49]. Although oxygen was not involved in this study, $MgCl_2$ treatment can be applied and is expected to have a minimally invasive therapeutic application. Trafermin,

used to treat bedsores and ulcers, is essential for preparing human fibroblast growth factors. It cannot be applied to cancerous ulcers because of concerns that it causes the proliferation of cancer cells [50]. Further studies are needed to clarify its applicability to cancerous ulcers, as the growth-promoting effect of Mg^{2+} treatment has also been reported [16].

In patients with diabetes mellitus, advanced glycation end products (AGEs) accumulate due to hyperglycemia, blood flow reduces due to arteriosclerosis, and immune cells are dysfunctional, thereby resulting in delayed wound healing and ulceration of the feet [51,52]. Notably, AGE accumulation in patients with diabetes mellitus suppressed the expression levels of MMP7 in the epidermal stem cells [53], suggesting that MMP7 may be important for wound healing processes. In addition, hypomagnesemia is prevalent in patients with diabetes, and peripheral neuropathy and abnormal platelet activity due to hypomagnesemia are risk factors for diabetic foot lesions [54]. Based on the above reports, appropriate maintenance of blood Mg^{2+} levels in diabetic patients might be valuable in preventing and treating diabetic foot lesions [55].

4. Materials and Methods

4.1. Cell Cultures

Human epidermal keratinocyte derived HaCaT cells were allocated by Prof. Tadamichi Shimizu (Department of Dermatology, Faculty of Medicine, University of Toyama) and cultured in Dulbecco's modified Eagle's medium containing 5% fetal bovine serum (FBS), 0.14 mg/mL streptomycin sulfate, and 0.07 mg/mL penicillin G potassium at 37 °C with 5% CO_2. Every 3–4 days, HaCaT cells were passaged using 0.02% ethylenediaminetetraacetic acid disodium salt (EDTA), phosphate-buffered saline (PBS), and 0.5% trypsin. NHEK cells were purchased from Kurabo (Tokyo, Japan). NHEK cells were cultured in a medium for keratinocytes (Lifeline Cell Technology, Frederick, MD, USA) at 37 °C with 5% CO_2.

4.2. RNA Extraction and Reverse Transcription Reaction

RNAzol RT Reagent was used in accordance with the manufacturer's instructions to extract total RNA from cells. Collected total RNA was dissolved in RNase-free water to make a total RNA sample. A reverse transcription reaction was then performed using a ReverTra Ace qPCR RT Kit (Toyobo, Osaka, Japan). The sample solution was incubated at 37 °C for 15 min, 50 °C for 15 min, and 95 °C for 5 min. After the reaction, the sample solution was used for real-time PCR.

4.3. Real-Time PCR

THUNDERBIRD Next SYBR qPCR Mix, primer pair, cDNA, and water were mixed. The PCR reaction was performed using Real-Time PCR Eco (As one, Tokyo, Japan) with three incubation steps as follows: (1) initial denaturation at 95 °C for 1 min; (2) annealing at 95 °C for 15 sec; and (3) elongation at 60 °C for 45 sec, all repeated for 40 cycles. After the PCR reaction, the growth and melting curves were analyzed to confirm non-specific reactions. When calibrated using some of the internal control genes, the changes in gene expression levels were similar. Therefore, β-actin was used as an internal standard for analysis. Primer sequences used in this study are presented in Table 1.

Table 1. Primer sequences used in real-time PCR.

Genes	Direction	Sequence (5′ → 3′)
DSG3	Forward	GACTCCTTCGGAAAGCAGCA
DSG3	Reverse	AAGCTTGGAGTTTCCTCCCG
FOSL2	Forward	GCCCAGTGTGCAAGATTAGC
FOSL2	Reverse	GGGCTCCTGTTTCACCACTA
LCE1E	Forward	TGAATAGCTGAGAGGTTCCAGC

Table 1. *Cont.*

Genes	Direction	Sequence (5′ → 3′)
LCE1E	Reverse	CAGCCATGGATCTGCAGAAG
MMP1	Forward	GGAGGAAATCTTGCTCAT
MMP1	Reverse	CTCAGAAAGAGCAGCATC
MMP2	Forward	ATGACGATGAGCTATGGACCTT
MMP2	Reverse	TCAGTGCAGCTGTTGTACTCCT
MMP7	Forward	TGTATGGGGAACTGCTGACA
MMP7	Reverse	GCGTTCATCCTCATCGAAGT
MMP9	Forward	TCTTCCAGTACCGAGAGAAAGC
MMP9	Reverse	GTCATAGGTCACGTAGCCCACT
SEMA3C	Forward	CAAAGATCCCACACACGGCT
SEMA3C	Reverse	ACTTGGTCCTCTGATCTCCTCC
SEMA5A	Forward	GTCTATACTTACTGCCAGCG
SEMA5A	Reverse	GTTAAATGCCTTGATGGCCTC
TP63	Forward	TTCTTAGCGAGGTTGGGCTG
TP63	Reverse	GATCGCATGTCGAAATTGCTC
WNT5A	Forward	CAATGAACCTACATAACAATGAAGC
WNT5A	Reverse	CAGCGGCAGTCTACTGACAT
β-Actin	Forward	CCTGAGGCACTCTTCCAGCCTT
β-Actin	Reverse	TGCGGATGTCCACGTCACACTTC
Filaggrin	Forward	GCAAGGTCAAGTCCAGGAGAA
Filaggrin	Reverse	CCCTCGGTTTCCACTGTCTC
Keratin-1	Forward	CAGACATGGGGATAGTGTGAGA
Keratin-1	Reverse	CAGGTCATTCAGCTTGTTCTTG
Loricrin	Forward	GGGCACCGATGGGCTTAG
Loricrin	Reverse	GGTAGGTTAAGACATGAAGGATTTGC
Involucrin	Forward	GGCCCTCAGATCGTCTCATA
Involucrin	Reverse	CACCCTCACCCCATTAAAGA
CyclinD1	Forward	TATTGCGCTGCTACCGTTGA
CyclinD1	Reverse	CCAATAGCAGCAAACAATGTGAAA

4.4. Scratch Assay

HaCaT cells were cultured in a 6-well plate to reach confluence. The cells were treated with 0.8–10.8 mM $MgCl_2$ or 5.8 mM $MgSO_4$. After 72 h incubation, the cells were incubated in serum-free medium for 16 h. After scratching with a pipette tip, bright field images of the cells were captured using a microscope (BZ810, Keyence, Osaka, Japan) at 0, 12, 18, and 24 h. A 0.5% FBS-containing medium was used during the recovery process to exclude the effects of cell proliferation. In the knockdown assay, HaCaT cells were transfected with a universal negative control and MMP7 siRNA using Lipofectamine RNAiMAX (Thermo Fisher Scientific, Waltham, MA, USA) for 48 h, and they were then used for the above scratch assay.

4.5. Sodium Dodecyl Sulfate (SDS)-Polyacrylamide Gel Electrophoresis (SDS-PAGE) and Western Blotting Analysis

HaCaT cells cultured in a 6-well plate were treated with 5.8 mM $MgCl_2$. In the Ca^{2+} chelating experiment, 50 μM BAPTA-AM (Dojindo) was treated for 0.5 h before $MgCl_2$ treatment. Cells were collected and added to a lysis buffer (150 mM NaCl, 1 mM EDTA, 20 mM Tris-HCl, 1% Triton X-100, 0.1% SDS, pH 7.4, protease inhibitor, phosphatase inhibitor cocktail, and 1% 2,2,2-trichloroethanol) and were disrupted by sonication (Bioruptor UCD-250, Cosmo Bio, Tokyo, Japan). After centrifugation at $6000 \times g$, the supernatant was collected as a cell lysate. The cell lysate was prepared in sample buffer containing SDS and bromophenol blue, and the proteins were denatured at 99.9 °C for 5 min. Electrophoresis was performed using a 10% or 12.5% acrylamide gel at 25 mA for approximately 90 min. After electrophoresis, the proteins were irradiated with UVB at 1 J/cm^2 in a UVP Crosslinker CL-1000M (Analytik Jena). The proteins were then transferred to polyvinylidene fluoride (PVDF) membranes in a semi-dry fashion at 100 mA for 60 min. After transfer, all protein bands were detected using LuminoGraph II (Atto, Tokyo, Japan) equipped with WUV-M20 UV Transilluminator. The membranes were immersed in a blocking solution (TBS-T containing 2% skim milk) and incubated at room temperature for 30 min. After removal of the blocking solution, the membrane was incubated with a primary antibody solution diluted (1:1000) in Solution 1 of Can Get Signal Immunoreaction Enhancer Solution (Toyobo) overnight at 4 °C. The following primary antibodies were used: anti-MMP7 antibody (A0695, ABclonal, MA, USA), anti-p-ERK1/2 antibody (sc-81492, Santa Cruz Biotechnology, TX, USA), and anti-ERK (p44/42 MAP kinase) antibody (#9102, Cell Signaling Technology, Danvers, MA, USA). The membranes were then incubated with horseradish peroxidase-conjugated secondary antibodies corresponding to the various primary antibodies for 90 min at room temperature. After treatment with the ECL detection reagents, the bands were detected using LuminoGraph II. Protein expression levels were corrected using total protein levels.

4.6. F-Actin Staining

The cells were stained with an F-actin-specific molecular probe, Phalloidin, to visualize the actin filaments in the early phase of cell migration, at 0, 1, and 6 h after scratching. After removal of the medium, cells were washed with PBS and fixed with 4% paraformaldehyde, permeabilized with 0.2% Triton X-100/PBS, and then incubated with the staining solution (100 nM rhodamine phalloidin and 572 nM DAPI) for 30 min. Fluorescence images of the stained cells were observed using Evos FL Auto 2 (Thermo Fisher Scientific).

4.7. Fluorescence Immunostaining

The cells were cultured in 6-well plates with a non-fluorescent cover glass placed at the bottom. After removal of the medium, the cells were washed with PBS, fixed with cold methanol at −30 °C, permeated with 0.2% Triton X-100/PBS at room temperature, blocked with 4% Block Ace for 30 min at room temperature, and reacted with the primary antibody (anti-MMP7 antibody) overnight at 4 °C. DAPI and the Alexa Fluor-546-labelled secondary antibody were reacted with the cells for 2 h, and the cover glass was then fixed on a glass slide with a mounting agent. Fluorescence immunostained cells were observed for fluorescence using a confocal laser microscope LSM 700 (Carl Zeiss, Jena, Germany). Images were captured using a $100 \times$ oil immersion objective on an inverted fluorescence microscope.

4.8. Statistical Analysis

Results are presented as mean $\pm$ standard error. Differences between groups were analyzed using one-way analysis of variance, and corrections for multiple comparisons were made using Dunnett's test or Tukey's multiple comparison test. Comparisons between the two groups were made using Student's *t*-test. Statistical analyses were performed using

the KaleidaGraph version 4.5.1 software (Synergy Software, Reading, PA, USA). Differences were considered to be significant at $p < 0.05$.

5. Conclusions

The mechanism of the wound healing-promoting action of $MgCl_2$ and $MgSO_4$ was investigated in the present study. The results revealed that $MgCl_2$ inhibits epidermal differentiation and promotes cell migration through the MEK/ERK/MMP7 pathway. Our data suggest that Mg^{2+} is expected to be indicated for medical treatment of early-stage wounds.

References

1. Proksch, E.; Brandner, J.M.; Jensen, J.M. The skin: An indispensable barrier. *Exp. Dermatol.* **2008**, *17*, 1063–1072. [CrossRef] [PubMed]
2. Coolen, N.A.; Schouten, K.C.W.M.; Middelkoop, E.; Ulrich, M.M.W. Comparison between human fetal and adult skin. *Arch. Dermatol. Res.* **2010**, *302*, 47–55. [CrossRef] [PubMed]
3. Nakamura, T.; Yoshitomi, Y.; Sakai, K.; Patel, V.; Fukumoto, S.; Yamada, Y. Epiprofin orchestrates epidermal keratinocyte proliferation and differentiation. *J. Cell Sci.* **2014**, *127*, 5261–5272. [CrossRef] [PubMed]
4. Werner, S.; Grose, R. Regulation of wound healing by growth factors and cytokines. *Physiol. Rev.* **2003**, *83*, 835–870. [CrossRef] [PubMed]
5. Kocaaga, B.; Kurkcuoglu, O.; Tatlier, M.; Dinler-Doganay, G.; Batirel, S.; Güner, F.S. Pectin-Zeolite-Based Wound Dressings with Controlled Albumin Release. *Polymers* **2022**, *14*, 460. [CrossRef]
6. Hultqvist, M.; Olsson, L.M.; Gelderman, K.A.; Holmdahl, R. The protective role of ROS in autoimmune disease. *Trends Immunol.* **2009**, *30*, 201–208. [CrossRef] [PubMed]
7. Harding, K.G.; Morris, H.L.; Patel, G.K. Science, medicine and the future: Healing chronic wounds. *BMJ* **2002**, *324*, 160–163. [CrossRef]
8. Reinartz, J.; Link, J.; Todd, R.F.; Kramer, M.D. The receptor for urokinase-type plasminogen activator of a human keratinocyte line (HaCaT). *Exp. Cell Res.* **1994**, *214*, 486–498. [CrossRef] [PubMed]
9. Gutiérrez-Fernández, A.; Inada, M.; Balbín, M.; Fueyo, A.; Pitiot, A.S.; Astudillo, A.; Hirose, K.; Hirata, M.; Shapiro, S.D.; Noël, A.; et al. Increased inflammation delays wound healing in mice deficient in collagenase-2 (MMP-8). *FASEB J.* **2007**, *21*, 2580–2591. [CrossRef]
10. Gipson, I.K.; Spurr-Michaud, S.J.; Tisdale, A.S. Hemidesmosomes and anchoring fibril collagen appear synchronously during development and wound healing. *Dev. Biol.* **1988**, *126*, 253–262. [CrossRef]
11. Lee, Y.I.; Shim, J.E.; Kim, J.; Lee, W.J.; Kim, J.W.; Nam, K.H.; Lee, J.H. WNT5A drives interleukin-6-dependent epithelial–mesenchymal transition via the JAK/STAT pathway in keloid pathogenesis. *Burn. Trauma.* **2022**, *10*, tkac023. [CrossRef] [PubMed]
12. Machesney, M.; Tidman, N.; Waseem, A.; Kirby, L.; Leigh, I. Activated keratinocytes in the epidermis of hypertrophic scars. *Am. J. Pathol.* **1998**, *152*, 1133–1141. [PubMed]
13. de Baaij, J.H.; Hoenderop, J.G.; Bindels, R.J. Magnesium in man: Implications for health and disease. *Physiol. Rev.* **2015**, *95*, 1–46. [CrossRef] [PubMed]
14. Akizawa, Y.; Koizumi, S.; Itokawa, Y.; Ojima, T.; Nakamura, Y.; Tamura, T.; Kusaka, Y. Daily Magnesium Intake and Serum Magnesium Concentration among Japanese People. *J. Epidemiol.* **2008**, *18*, 151–159. [CrossRef] [PubMed]
15. Lacapère, J.J.; Bennett, N.; Dupont, Y.; Guillain, F. pH and magnesium dependence of ATP binding to sarcoplasmic reticulum ATPase. Evidence that the catalytic ATP-binding site consists of two domains. *J. Biol. Chem.* **1990**, *265*, 348–353. [CrossRef]

16. Cappadone, C.; Malucelli, E.; Zini, M.; Farruggia, G.; Picone, G.; Gianoncelli, A.; Notargiacomo, A.; Fratini, M.; Pignatti, C.; Iotti, S.; et al. Assessment and Imaging of Intracellular Magnesium in SaOS-2 Osteosarcoma Cells and Its Role in Proliferation. *Nutrients* **2021**, *13*, 1376. [CrossRef]

17. Hammamieh, R.; Yang, D.C.H. Magnesium Ion-mediated Binding to tRNA by an Amino-terminal Peptide of a Class II tRNA Synthetase. *J. Biol. Chem.* **2001**, *276*, 428–433. [CrossRef] [PubMed]

18. Wolf, F.I.; Cittadini, A. Magnesium in cell proliferation and differentiation. *Front. Biosci.* **1999**, *4*, D607–D617. [CrossRef]

19. Marunaka, K.; Shu, S.; Kobayashi, M.; Goto, M.; Katsuta, Y.; Yoshino, Y.; Ikari, A. Elevation of Hyaluronan Synthase by Magnesium Supplementation Mediated through the Activation of GSK3 and CREB in Human Keratinocyte-Derived HaCaT Cells. *Int. J. Mol. Sci.* **2021**, *23*, 71. [CrossRef]

20. Shu, S.; Kobayashi, M.; Marunaka, K.; Yoshino, Y.; Goto, M.; Katsuta, Y.; Ikari, A. Magnesium Supplementation Attenuates Ultraviolet-B-Induced Damage Mediated through Elevation of Polyamine Production in Human HaCaT Keratinocytes. *Cells* **2022**, *11*, 2268. [CrossRef]

21. Denda, M.; Katagiri, C.; Hirao, T.; Maruyama, N.; Takahashi, M. Some magnesium salts and a mixture of magnesium and calcium salts accelerate skin barrier recovery. *Arch. Dermatol. Res.* **1999**, *291*, 560–563. [CrossRef] [PubMed]

22. Yang, F.; Xue, Y.; Wang, F.; Guo, D.; He, Y.; Zhao, X.; Yan, F.; Xu, Y.; Xia, D.; Liu, Y. Sustained release of magnesium and zinc ions synergistically accelerates wound healing. *Bioact. Mater.* **2023**, *26*, 88–101. [CrossRef] [PubMed]

23. Koster, M.I.; Dai, D.; Marinari, B.; Sano, Y.; Costanzo, A.; Karin, M.; Roop, D.R. p63 induces key target genes required for epidermal morphogenesis. *Proc. Natl. Acad. Sci. USA* **2007**, *104*, 3255–3260. [CrossRef] [PubMed]

24. Kurata, S.; Okuyama, T.; Osada, M.; Watanabe, T.; Tomimori, Y.; Sato, S.; Iwai, A.; Tsuji, T.; Ikawa, Y.; Katoh, I. p51/p63 Controls subunit alpha3 of the major epidermis integrin anchoring the stem cells to the niche. *J. Biol. Chem.* **2004**, *279*, 50069–50077. [CrossRef] [PubMed]

25. Schmitt, T.; Pircher, J.; Steinert, L.; Meier, K.; Ghoreschi, K.; Vielmuth, F.; Kugelmann, D.; Waschke, J. Dsg1 and Dsg3 Composition of Desmosomes Across Human Epidermis and Alterations in Pemphigus Vulgaris Patient Skin. *Front. Immunol.* **2022**, *13*, 884241. [CrossRef]

26. Ishitsuka, Y.; Huebner, A.J.; Rice, R.H.; Koch, P.J.; Speransky, V.V.; Steven, A.C.; Roop, D.R. Lce1 Family Members Are Nrf2-Target Genes that Are Induced to Compensate for the Loss of Loricrin. *J. Invest. Dermatol.* **2016**, *136*, 1656–1663. [CrossRef] [PubMed]

27. Wurm, S.; Zhang, J.; Guinea-Viniegra, J.; García, F.; Muñoz, J.; Bakiri, L.; Ezhkova, E.; Wagner, E.F. Terminal epidermal differentiation is regulated by the interaction of Fra-2/AP-1 with Ezh2 and ERK1/2. *Genes. Dev.* **2015**, *29*, 144–156. [CrossRef] [PubMed]

28. Lim, X.; Tan, S.H.; Koh, W.L.C.; Chau, R.M.W.; Yan, K.S.; Kuo, C.J.; Van Amerongen, R.; Klein, A.M.; Nusse, R. Interfollicular Epidermal Stem Cells Self-Renew via Autocrine Wnt Signaling. *Science* **2013**, *342*, 1226–1230. [CrossRef] [PubMed]

29. Romanowska, M.; Evans, A.; Kellock, D.; Bray, S.E.; Mclean, K.; Donandt, S.; Foerster, J. Wnt5a Exhibits Layer-Specific Expression in Adult Skin, Is Upregulated in Psoriasis, and Synergizes with Type 1 Interferon. *PLoS ONE* **2009**, *4*, e5354. [CrossRef]

30. Kurokawa, I.; Mizutani, H.; Kusumoto, K.; Nishijima, S.; Tsujita-Kyutoku, M.; Shikata, N.; Tsubura, A. Cytokeratin, filaggrin, and p63 expression in reepithelialization during human cutaneous wound healing. *Wound Repair. Regen.* **2006**, *14*, 38–45. [CrossRef]

31. Lu, B.; Rothnagel, J.A.; Longley, M.A.; Tsai, S.Y.; Roop, D.R. Differentiation-specific expression of human keratin 1 is mediated by a composite AP-1/steroid hormone element. *J. Biol. Chem.* **1994**, *269*, 7443–7449. [CrossRef] [PubMed]

32. Nemes, Z.; Steinert, P.M. Bricks and mortar of the epidermal barrier. *Exp. Mol. Med.* **1999**, *31*, 5–19. [CrossRef] [PubMed]

33. Nithya, S.; Radhika, T.; Jeddy, N. Loricrin—An overview. *J. Oral. Maxillofac. Pathol.* **2015**, *19*, 64–68. [CrossRef] [PubMed]

34. Sano, T.; Kobayashi, T.; Ogawa, O.; Matsuda, M. Gliding Basal Cell Migration of the Urothelium during Wound Healing. *Am. J. Pathol.* **2018**, *188*, 2564–2573. [CrossRef] [PubMed]

35. Rottner, K.; Stradal, T.E. Actin dynamics and turnover in cell motility. *Curr. Opin. Cell Biol.* **2011**, *23*, 569–578. [CrossRef] [PubMed]

36. Roy, M.; Li, Z.; Sacks, D.B. IQGAP1 Is a Scaffold for Mitogen-Activated Protein Kinase Signaling. *Mol. Cell. Biol.* **2005**, *25*, 7940–7952. [CrossRef] [PubMed]

37. Mu, N.; Gu, J.; Liu, N.; Xue, X.; Shu, Z.; Zhang, K.; Huang, T.; Chu, C.; Zhang, W.; Gong, L.; et al. PRL-3 is a potential glioblastoma prognostic marker and promotes glioblastoma progression by enhancing MMP7 through the ERK and JNK pathways. *Theranostics* **2018**, *8*, 1527–1539. [CrossRef] [PubMed]

38. Rohani, M.G.; Pilcher, B.K.; Chen, P.; Parks, W.C. Cdc42 Inhibits ERK-Mediated Collagenase-1 (MMP-1) Expression in Collagen-Activated Human Keratinocytes. *J. Investig. Dermatol.* **2014**, *134*, 1230–1237. [CrossRef] [PubMed]

39. Wang, J.; Wang, C.; Li, Q.; Guo, C.; Sun, W.; Zhao, D.; Jiang, S.; Hao, L.; Tian, Y.; Liu, S.; et al. miR-429-CRKL axis regulates clear cell renal cell carcinoma malignant progression through SOS1/MEK/ERK/MMP2/MMP9 pathway. *Biomed. Pharmacother.* **2020**, *127*, 110215. [CrossRef]

40. Mammoli, F.; Castiglioni, S.; Parenti, S.; Cappadone, C.; Farruggia, G.; Iotti, S.; Davalli, P.; Maier, J.; Grande, A.; Frassineti, C. Magnesium Is a Key Regulator of the Balance between Osteoclast and Osteoblast Differentiation in the Presence of Vitamin D3. *Int. J. Mol. Sci.* **2019**, *20*, 385. [CrossRef]

41. Zocchi, M.; Locatelli, L.; Zuccotti, G.V.; Mazur, A.; Béchet, D.; Maier, J.A.; Castiglioni, S. Magnesium Homeostasis in Myogenic Differentiation—A Focus on the Regulation of TRPM7, MagT1 and SLC41A1 Transporters. *Int. J. Mol. Sci.* **2022**, *23*, 1658. [CrossRef] [PubMed]

42. Kamata, Y.; Tominaga, M.; Umehara, Y.; Honda, K.; Kamo, A.; Moniaga, C.S.; Komiya, E.; Toyama, S.; Suga, Y.; Ogawa, H.; et al. Calcium-Inducible MAPK/AP-1 Signaling Drives Semaphorin 3A Expression in Normal Human Epidermal Keratinocytes. *J. Investig. Dermatol.* **2020**, *140*, 1346–1354.e1345. [CrossRef] [PubMed]

43. Luo, J.; Stewart, R.; Berdeaux, R.; Hu, H. Tonic inhibition of TRPV3 by Mg2+ in mouse epidermal keratinocytes. *J. Invest. Dermatol.* **2012**, *132*, 2158–2165. [CrossRef] [PubMed]

44. Harmon, R.M.; Simpson, C.L.; Johnson, J.L.; Koetsier, J.L.; Dubash, A.D.; Najor, N.A.; Sarig, O.; Sprecher, E.; Green, K.J. Desmoglein-1/Erbin interaction suppresses ERK activation to support epidermal differentiation. *J. Clin. Investig.* **2013**, *123*, 1556–1570. [CrossRef] [PubMed]

45. Caley, M.P.; Martins, V.L.C.; O'Toole, E.A. Metalloproteinases and Wound Healing. *Adv. Wound Care* **2015**, *4*, 225–234. [CrossRef] [PubMed]

46. Amir, M.; Romano, S.; Goldman, S.; Shalev, E. Plexin-B1, glycodelin and MMP7 expression in the human fallopian tube and in the endometrium. *Reprod. Biol. Endocrinol.* **2009**, *7*, 152. [CrossRef] [PubMed]

47. Ding, K.; Lopez-Burks, M.; Sánchez-Duran, J.A.; Korc, M.; Lander, A.D. Growth factor-induced shedding of syndecan-1 confers glypican-1 dependence on mitogenic responses of cancer cells. *J. Cell Biol.* **2005**, *171*, 729–738. [CrossRef] [PubMed]

48. Ikari, A.; Kinjo, K.; Atomi, K.; Sasaki, Y.; Yamazaki, Y.; Sugatani, J. Extracellular Mg(2+) regulates the tight junctional localization of claudin-16 mediated by ERK-dependent phosphorylation. *Biochim. Biophys. Acta* **2010**, *1798*, 415–421. [CrossRef]

49. Oyebode, O.A.; Jere, S.W.; Houreld, N.N. Current Therapeutic Modalities for the Management of Chronic Diabetic Wounds of the Foot. *J. Diabetes Res.* **2023**, *2023*, 1–10. [CrossRef]

50. Ueno, K.; Takeuchi, Y.; Samura, M.; Tanaka, Y.; Nakamura, T.; Nishimoto, A.; Murata, T.; Hosoyama, T.; Hamano, K. Treatment of refractory cutaneous ulcers with mixed sheets consisting of peripheral blood mononuclear cells and fibroblasts. *Sci. Rep.* **2016**, *6*, 28538. [CrossRef]

51. Falanga, V. Wound healing and its impairment in the diabetic foot. *Lancet* **2005**, *366*, 1736–1743. [CrossRef] [PubMed]

52. Tsourdi, E.; Barthel, A.; Rietzsch, H.; Reichel, A.; Bornstein, S.R. Current aspects in the pathophysiology and treatment of chronic wounds in diabetes mellitus. *Biomed. Res. Int.* **2013**, *2013*, 385641. [CrossRef] [PubMed]

53. Zhu, J.; Wang, P.; Yu, Z.; Lai, W.; Cao, Y.; Huang, P.; Xu, Q.; Yu, M.; Xu, J.; Huang, Z.; et al. Advanced glycosylation end product promotes forkhead box O1 and inhibits Wnt pathway to suppress capacities of epidermal stem cells. *Am. J. Transl. Res.* **2016**, *8*, 5569–5579.

54. Razzaghi, R.; Pidar, F.; Momen-Heravi, M.; Bahmani, F.; Akbari, H.; Asemi, Z. Magnesium Supplementation and the Effects on Wound Healing and Metabolic Status in Patients with Diabetic Foot Ulcer: A Randomized, Double-Blind, Placebo-Controlled Trial. *Biol. Trace Elem. Res.* **2018**, *181*, 207–215. [CrossRef] [PubMed]

55. Piuri, G.; Zocchi, M.; Della Porta, M.; Ficara, V.; Manoni, M.; Zuccotti, G.V.; Pinotti, L.; Maier, J.A.; Cazzola, R. Magnesium in Obesity, Metabolic Syndrome, and Type 2 Diabetes. *Nutrients* **2021**, *13*, 320. [CrossRef] [PubMed]